Subwavelength-resolution imaging of surface plasmon polaritons with up-conversion fluorescence microscopy: supplement

LAM YEN THI NGUYEN, YI-HSIN LEE, YU-FANG CHANG, CHIA-CHEN HSU, JIUNN-YUAN LIN, AND HUNG-CHIH KAN [ID]

Department of Physics, National Chung Cheng University, 168, Sec. 1, University Road, Min-Hsiung, Chiayi 621, Taiwan
*phyhck@ccu.edu.tw

Subwavelength-Resolution Imaging of Surface Plasmon Polaritons with Up-Conversion Fluorescent Microscopy: supplemental document
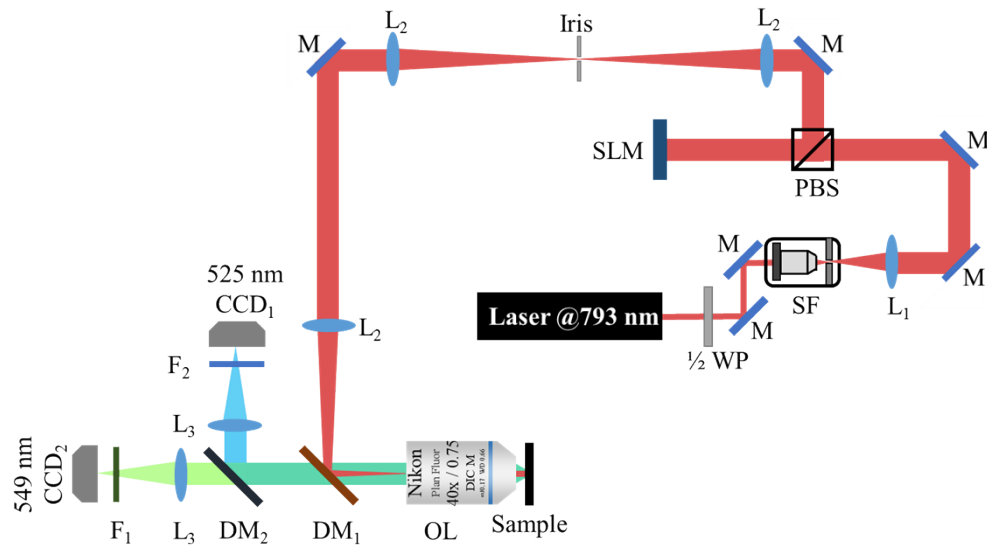

Fig. S1. The schematics of the experimental setup of the up-conversion fluorescent microscopy.
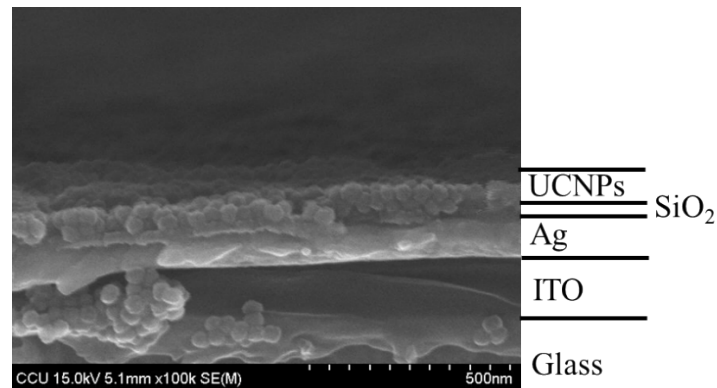

Fig. S2. The field emission scanning electron microscope (FESEM) image of a cross-sectional view of the sample with spin-coated UCNPs. The thickness of the layers as labelled from top to bottom is: ~ 50nm for UCNPs layer, 20 nm for SiO_2 layer, 100 nm for Ag film, and ~240nm for ITO coating.

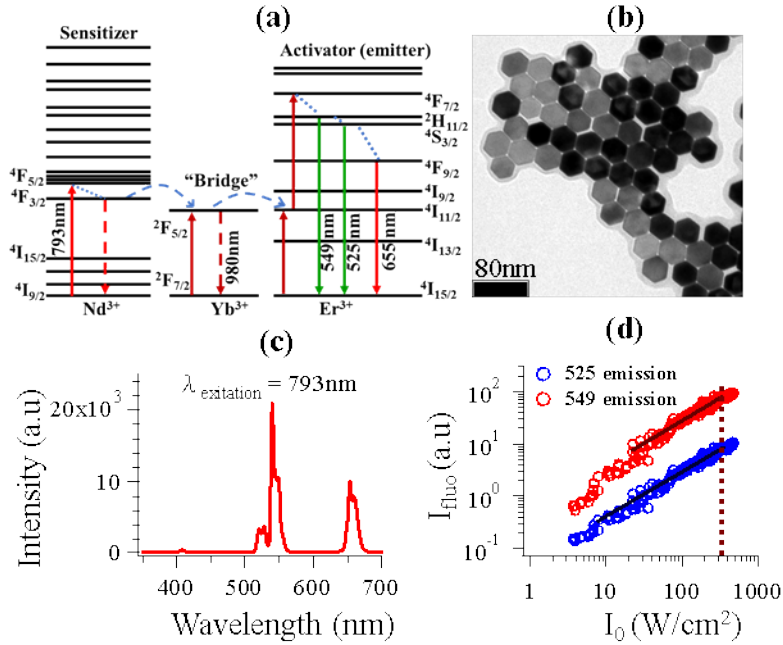Figure S3. (a) Schematic illustration of the energy diagram of the core-shell-shell $NaYF_4:Yb^{3+}$, Er^{3+} @ $NaYF_4:Yb^{3+}$, Nd^{3+} @ $NaYF_4$ Core@Shell@Shell UCNPs. Nd^{3+} ions in the inner shell are the sensitizer which absorb the energy of the 793 nm wavelength photons of the incident light, then transfer energy to Yb^{3+} ions through the resonant energy transfer process. The excited Yb^{3+} ions then transfer energy to Er^{3+} ions in the core. (b) Transmission electron microscopy (TEM) image of UCNPs $NaYF_4:Yb^{3+}$, Er^{3+}@ $NaYF_4:Nd^{3+}$, Yb^{3+}@ $NaYF_4$ with average size of 49±2 nm. (c) The fluorescent emission spectra of the UCNPs under 793nm excitation. The major emission signals used for this experiment are the fluorescent emission at 525 nm, 549 nm wavelengths. (d) The incident intensity dependence of the 525nm and 549nm wavelength fluorescent emission intensities of the UCNPs spin-coated on the SiO_2/Ag substrate. The measurement was carried out with the fluorescent microscope at the flat area of the sample shown in Fig. 1. The red (blue) circles represent the 549nm (525nm) wavelength fluorescent emission results. The solid black lines are the results of the power law fitting to the major part of the data. The functional form of the fitting is $I_f = a \times I^b$, where I_f is the fluorescent intensity, I the excitation light intensity, a and b are the fitting constants. The power law exponents b are 0.86±0.02 and 0.81±0.02 for the 549 nm and 525 nm wavelength emission intensities, respectively. The vertical dashed line indicates the incident intensity used for the experimental results reported in the paper.
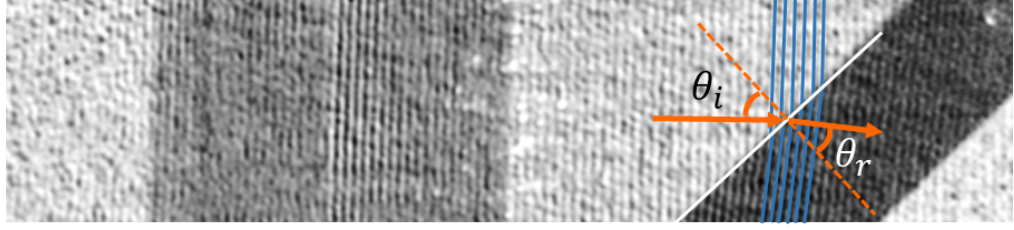
Figure S4. The scheme for the analysis of the incident and refraction angles for SPP refraction in Fig. 4a. The arrows represent the direction of the propagation of the SPPs, which are locally perpendicular to the fringes (highlighted with the blue line segments). The dashed line indicates the direction normal to the edge of the SiO_2 pad, which is highlighted with the white solid line. The angles θ_i and θ_r are the incident angle and the refraction angle, respectively, of the SPP refraction occurred at the left boundary of the SiO_2 pad.
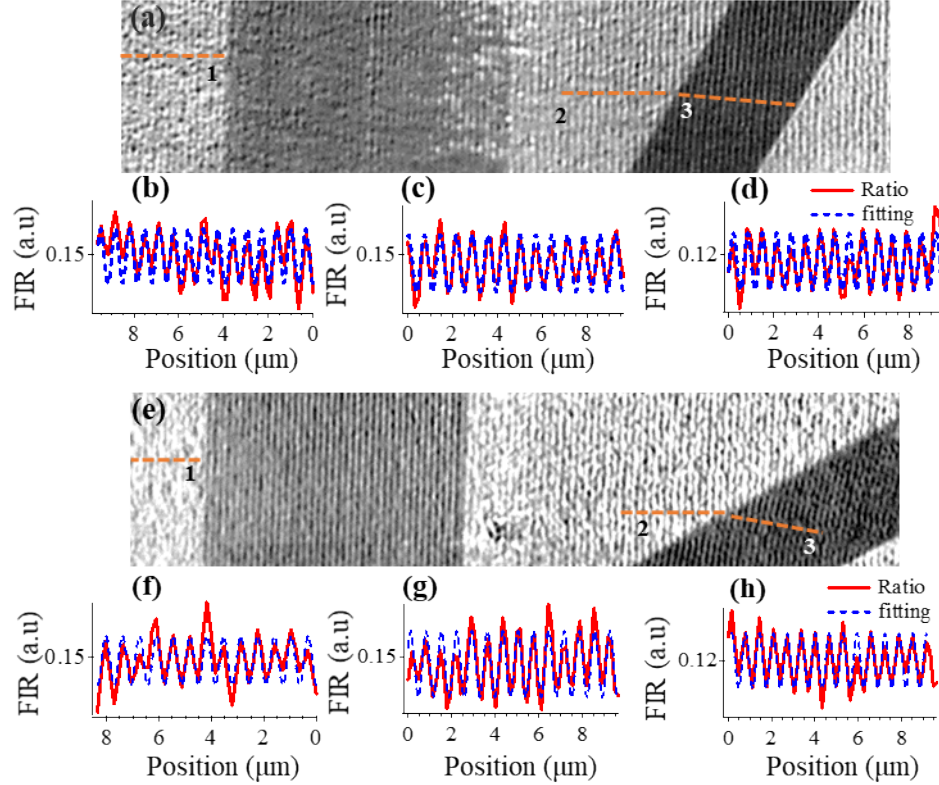

Fig. S5. (a) and (e) are the FIR images of the sample structure with the long edges of the SiO_2 pad at 30º and 60º azimuthal orientation, respectively. (b), (c), and (d) are the line profiles extracted from the image in panel (a) at position indicated with the dashed line segments labelled "1", "2", and "3", respectively. Similarly, (f), (g), and (h) are the line profiles extracted from the image in panel (e) at position indicated with the dashed line segments labelled "1", "2", and "3", respectively. The red solid curves in panels (b)-(c) and (f)-(h) represent the line profiles extracted from the images and the blue dashed curves are the results of fitting the line profiles to a sinusoidal function.
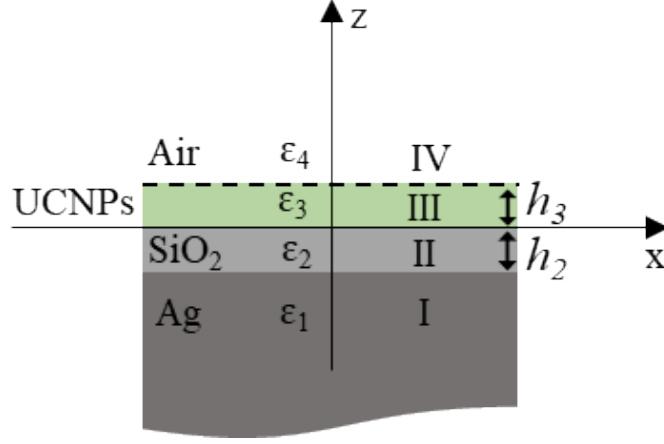
Air ε_4 IV

UCNPs ε_3 III $\updownarrow h_3$

SiO$_2$ ε_2 II $\updownarrow h_2$ x

Ag ε_1 I

z

Fig. S6. The boundary conditions that simulate the SPP propagation at the SiO$_2$/Ag interface in the experiment. ε_1, ε_2, ε_3, and ε_4 represent the dielectric constants of the Ag in layer I, the SiO$_2$ in layer II, the UNCPs in layer III, and the Air in region IV, respectively. The equations for the SPP wavevector k_x derived from the Maxwell's equations and the boundary conditions are the following.

$$a_2^2 a_3^2 \left(\frac{k_{z_1}}{\varepsilon_1} - \frac{k_{z_2}}{\varepsilon_2}\right)\left(\frac{k_{z_3}}{\varepsilon_3} - \frac{k_{z_4}}{\varepsilon_4}\right)\left(\frac{k_{z_2}}{\varepsilon_2} + \frac{k_{z_3}}{\varepsilon_3}\right) + a_2^2 \left(\frac{k_{z_1}}{\varepsilon_1} - \frac{k_{z_2}}{\varepsilon_2}\right)\left(\frac{k_{z_3}}{\varepsilon_3} + \frac{k_{z_4}}{\varepsilon_4}\right)\left(\frac{k_{z_2}}{\varepsilon_2} - \frac{k_{z_3}}{\varepsilon_3}\right)$$

$$+ a_3^2 \left(\frac{k_{z_1}}{\varepsilon_1} + \frac{k_{z_2}}{\varepsilon_2}\right)\left(\frac{k_{z_3}}{\varepsilon_3} - \frac{k_{z_4}}{\varepsilon_4}\right)\left(\frac{k_{z_2}}{\varepsilon_2} - \frac{k_{z_3}}{\varepsilon_3}\right) + \left(\frac{k_{z_1}}{\varepsilon_1} + \frac{k_{z_2}}{\varepsilon_2}\right)\left(\frac{k_{z_3}}{\varepsilon_3} + \frac{k_{z_4}}{\varepsilon_4}\right)\left(\frac{k_{z_2}}{\varepsilon_2} + \frac{k_{z_3}}{\varepsilon_3}\right) = 0 \quad (S1)$$

$$k_{z_1}^2 + k_x^2 = \varepsilon_1 \left(\frac{\omega}{c}\right)^2 \quad (S2)$$

$$k_{z_2}^2 + k_x^2 = \varepsilon_2 \left(\frac{\omega}{c}\right)^2 \quad (S3)$$

$$k_{z_3}^2 + k_x^2 = \varepsilon_3 \left(\frac{\omega}{c}\right)^2 \quad (S4)$$

$$k_{z_4}^2 + k_x^2 = \varepsilon_4 \left(\frac{\omega}{c}\right)^2 \quad (S5)$$

,where $a_2 = e^{ik_{z2}h_2}$,h_2 is thickness of the SiO$_2$ layer; $a_3 = e^{ik_{z3}h_3}$;,and h_3 = 50 nm for the effective thickness of the UCNP layer, k_{z1}, k_{z2}, k_{z3}, k_{z4} are the vertical components of the wave vectors of the electro-magnetic fields in regions I, II, III, and IV, respectively.
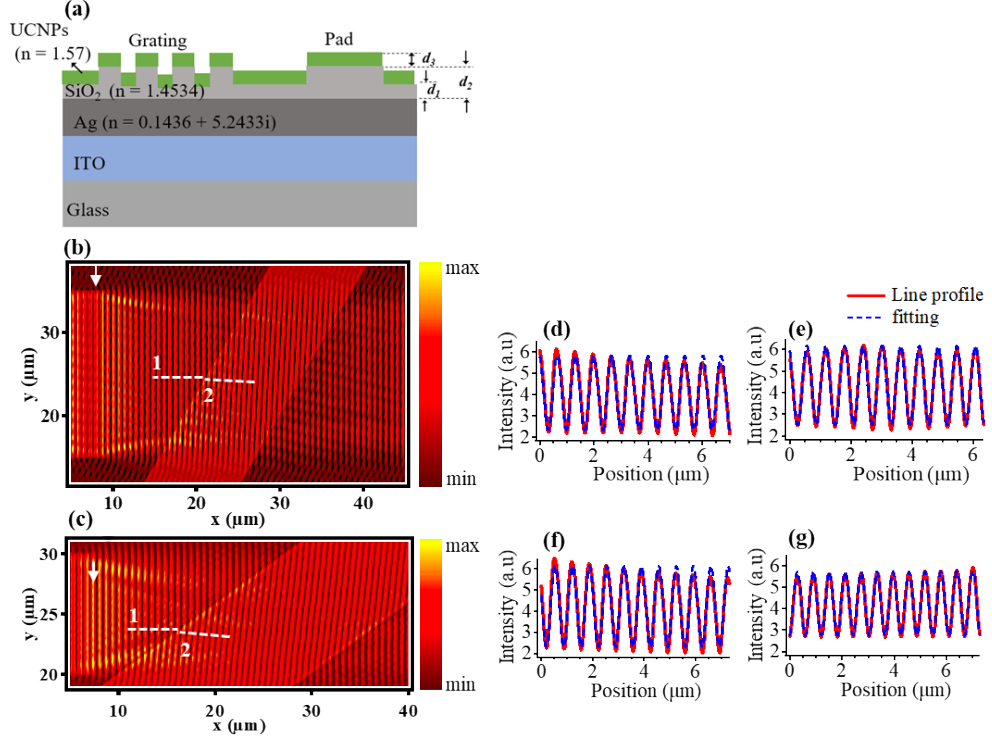
Fig. S7. The 3D-FDTD of the SPPs refraction. (a) the cross-sectional view of the model for the simulation. d_1 = 20 nm, d_2 = 60 nm, and d_3 = 50 nm. (b) and (c) show the E-field intensity at the plane 10nm above the SiO_2 structures plotted as a function of the lateral position for the cases of the SiO_2 pads with azimuth angle of 30º, 60º, respectively. The vertical arrows near the left edge of the images indicate the right edge of the grating structures. (d) and (e) show the intensity profiles (red solid lines) extracted from the image in (a) at positions indicated with the dashed line segments, labelled "1" and "2", respectively. The blue dashed lines are the results of fitting the line profiles to a sinusoidal function. Similarly, (f) and (g) show the intensity line profiles (red solid lines) extracted from the image in (b) at positions indicated with the dashed line segments, labelled "1" and "2", respectively. The blue dashed lines are the results of fitting the line profiles to a sinusoidal function.